THE RESULTS OF THE SPECIALISTS' AND SCIENTISTS' RESEARCHES

Original article
https://doi.org/10.15828/2075-8545-2024-16-4-361-374

Nanostructural changes in the components of chrysotile-cement dust under the influence of different levels of acidity and exposure time

Sergey V. Klyuev[1, 2]*, Lyudmila N. Naumova[2], Igor V. Nedoseko[3], Alexander V. Klyuev[2], Elena S. Shorstova[2]

[1] Peoples' Friendship University of Russia named after Patrice Lumumba, Moscow, Russia
[2] Belgorod State Technological University named after V.G. Shukhov, Belgorod, Russia
[3] Ufa State Petroleum Technological University, Ufa, Russia

* Corresponding author: e-mail: klyuyev@yandex.ru

ABSTRACT

Introduction. The article considers the issue of modifying the initial chrysotile fiber and its bundles by the action of hydration products of Portland cement and various acidity value of the treated medium. A brief justification of the relevance of the research topic is provided. It is noted that recently, issues of production of composite materials based on natural and man-made raw materials, which are a promising area of modern economics, have aroused great scientific and practical interest. The availability and low cost of raw materials, as well as low energy, transportation, and overhead costs, contribute to reducing the cost of composite materials. At the same time, the high contractual prices and strong demand in both domestic and foreign markets provide incentives for increasing production volumes. The aim of the research is to study the behavior of the initial chrysotile fibers and their aggregates in the composition of the cement component under the influence of different acidity of the treated medium. Research objective: to investigate the behavior of chrysotile cement dust components under an aggressive environmental condition with electron microscopy examination; calculation of the number and dimensional characteristics of nanofibers and dust particles under the influence of various exposure times of the aggressive factor; microdifraction studies of the nanostructure of the studied samples after exposure to acidic media. Materials and methods. The materials used in the research and their characteristics are given, in particular, chrysotile cement dust containing fibers of commercial chrysotile, acidity of the medium, exposure time, micro- and nanofibers obtained after exposure to aggressive medium. Samples of chrysotile cement dust were taken at the slate production No.1 of JSC "BelACI" and collected at the place of sawing of chrysotile cement products, underwent the stage of dispersion using a centrifugal separator. In the work chrysotile cement dust was used as an object of environmental pollution and its further use in the production of composite chrysotile cement products. **Results.** The results of studies on the influence of aggressive environment on the components of chrysotile-cement dust, their size characteristics, and structural nano-changes are presented. The studied samples have been examined in a scanning ion-electron microscope at magnifications of 200x, 500x, 5000x, 10000x, and their chemical composition have been analyzed. **Discussion.** The results of analysis of the obtained experimental data are given. Quantitative composition of fibers and aggregates of fibers in chrysotile cement dust changes after its exposure in acidic medium in comparison with their quantity in initial chrysotile cement dust, and the quantity of separate thin fibers increases, it is explained by the fact that in acidic medium there is not only destruction of cement stone, but also splitting of bundles of chrysotile fibers into micro- and nanofibers. **Conclusions.** Electron microscopic examination of initial commercial chrysotile fibers and their bundles in cement dust have shown changes in their dimensional and quantitative characteristics, including the products of Portland cement hydration under the influence of the factor of aggressiveness of the environment.

KEYWORDS: commercial chrysotile, chrysotile cement dust, micro- and nanofibers, hydration products, acidity of the medium, quantitative and dimensional characteristics.

ACKNOWLEDGMENTS: This work was supported by funding under the national project "Science and University" for the establishment of a new laboratory, "Development, Research, and Pilot-Industrial Testing of High-Tech Technologies and Technical Means for the Production of Polymer-Containing Composite Mixtures and Products from Technogenic Organomineral Components" (project FZWN 2024-0002).

This work was carried out using the equipment of the High Technology Center at V.G. Shukhov Belgorod State Technological University.

FOR CITATION:
Klyuev S.V., Naumova L.N., Nedoseko I.V., Klyuev A.V., Shorstova E.S. Nanostructural changes in the components of chrysotile-cement dust under the influence of different levels of acidity and exposure time. *Nanotechnologies in Construction.* 2024; 16(4): 361–374. https://doi.org/10.15828/2075-8545-2024-16-4-361-374. – EDN: IXRKHR.

INTRODUCTION

Chrysotile, formerly known as asbestos, is one of the most common minerals [1–3] in the group of serpentine silicates [4]. It possesses unique physical [5–8] and chemical properties [9–11], which make it valuable in many industrial applications. Chrysotile consists of fibers that can be thin, flexible, and have high tensile strength [12]. Its chemical formula can be represented as $Mg_3(Si_2O_5)(OH)4Mg_3(Si_2O_5)(OH)_4$, indicating its magnesium silicate composition with hydroxyl groups [13–15]. Due to its strength, high temperature resistance, and chemical inertness, chrysotile has found wide use in construction, automotive manufacturing, and other industries. In natural conditions, it forms three types of structures: cross-fibrous, longitudinal-fibrous, and tangled-fibrous. Fibers typically range from 2 to 5 mm in length [16], sometimes longer, up to 20–30 mm [17], and extremely rarely over 100 mm [18].

In industry, chrysotile is valued for its exceptional mechanical strength [19], low electrical conductivity [20,21], thermal stability [22], and excellent adsorption qualities [23]. Fiber length [24] plays a crucial role in its industrial applications. Approximately 60% of mined chrysotile is used in the production of chrysotile cement products, which, due to their unique properties, are widely used in the construction industry and other sectors. Chrysotile cement products include materials such as roofing and wall panels, pipes [25] for water supply and sewage [26], as well as various types of sheets and boards [27]. These products are valued for their strength [28], fire resistance, and durability [29], making them a popular choice for many construction projects [30,31].

The peak of chrysotile production [32–34] was reached in 1977, when the total production volume was approximately 5.5 million tons, with over 2.5 million tons from the USSR [35] and over 1.5 million tons from Canada [36]. Since the 1980s, due to environmental risks, chrysotile production volumes began to decline, dropping to 2 million tons by 1998 [37]. Today, the main producers of chrysotile are Russia, Canada, China, Brazil, Zimbabwe [38], Kazakhstan, and South Africa. The total asbestos reserves are estimated to be around 80 million tons, with chrysotile accounting for over 95% of this.

Industrial deposits of chrysotile, also known as white asbestos, often form as a result of hydrothermal and metamorphic processes [39–41], which significantly influence the formation and distribution of these minerals.

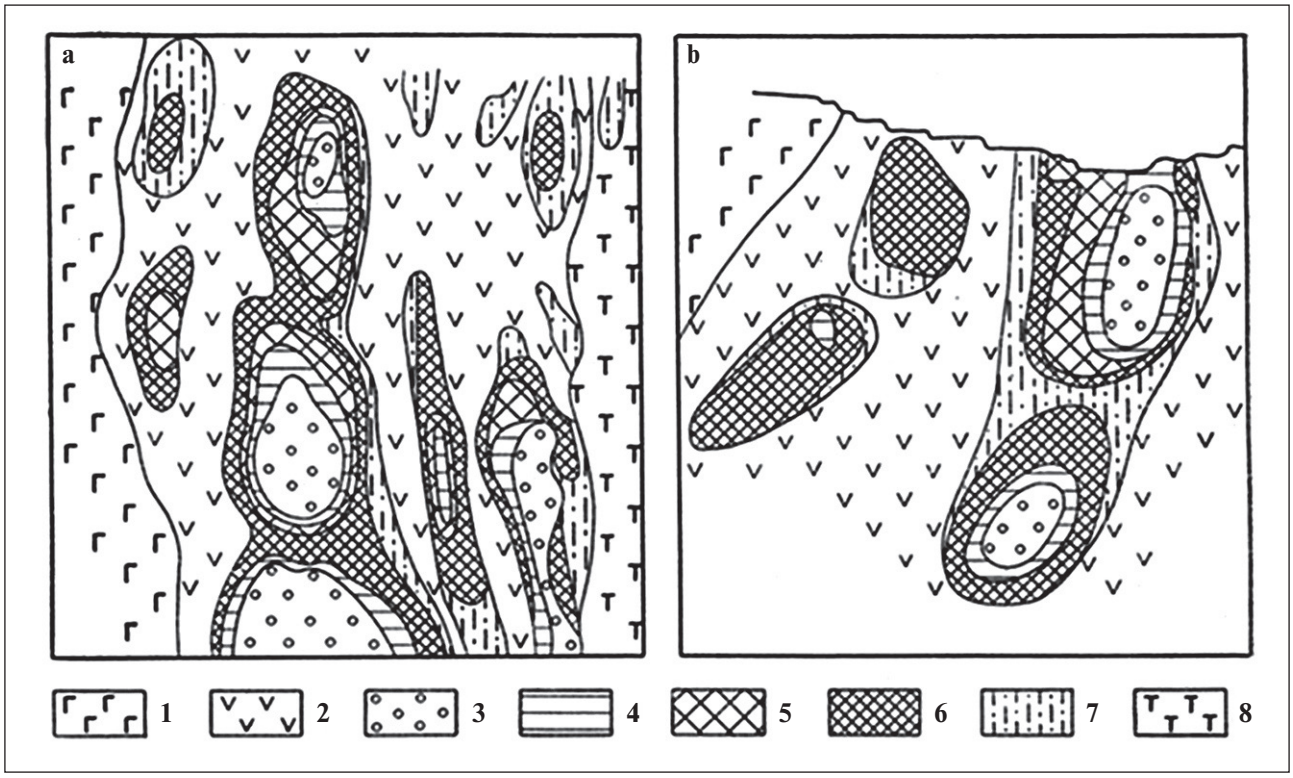

Fig. 1. **Schematic geological map (a) and cross-section (b) of a section of the Bazhenovskoye chrysotile deposit. According to V.F. Dybkov and M.M. Trapeznikova:** 1 – gabbro; 2 – serpentinites; 3 – peridotites; 4 – peridotites with bordered chrysotile veins; 5 – peridotites and serpentinites with coarse-mesh asbestos mineralization; 6 – serpentinites with fine-mesh asbestos mineralization and "fine-vein" chrysotile; 7 – serpentinites with chrysotile veining; 8 – talcified serpentinites

Hydrothermal processes involve the movement of hot aqueous solutions through cracks and pores in the Earth's crust, leading to changes in the chemical composition of surrounding rocks and the formation of new minerals. In the case of chrysotile, these processes can contribute to the enrichment of rocks with magnesium, a key component of the mineral. Metamorphic processes include the transformation of minerals under high temperatures and pressures, which is also characteristic of zones where chrysotile is found. These processes can lead to the serpentinization of ultramafic rocks, resulting in serpentine minerals, including chrysotile. The most significant industrial deposits belong to the apo-ultramafic type, which includes three subtypes: Bazhenovskoye, Labinskoye, and Karachayevo.

Bazhenov-type asbestos deposits belong to a special category characterized by certain geological and mineralogical features. These deposits are typically associated with the Bazhenov Suite, which is known for its unique black shales rich in organic matter. Bazhenov-type asbestos can contain various forms of asbestos minerals, including chrysotile and amphiboles. The uniqueness of these deposits lies in their concentric zonal structure, defined by a wide range of asbestos formations, varying from thin layers to single and complex bordered veins. A distinctive feature of these deposits is their concentric zoning, resulting from the diversity of asbestos occurrences, from thin interlayers to simple and complex bordered veins. This structure indicates a multi-level and complex nature of the processes that led to their formation, including both geological and hydrothermal influences. This gives Bazhenov deposits special value not only in the context of asbestos mining but also in terms of understanding the geological evolution of the region (Fig. 2).

The primary asbestos veins, rich in pure chrysotile with a cross-fiber structure [42], play a crucial role in asbestos deposits. These veins are found surrounded by massive serpentinites [43], followed by zones of serpentinized ultramafics [44], progressing to weakly serpentinized peridotites [45] or dunites [46]. These primary veins can contain asbestos fibers reaching lengths of up to 60 mm, which is considered significant for asbestos fibers [47].

More complex veins are characterized by the presence of multiple parallel asbestos veinlets separated by solid serpentinite. Although the fibers in these veins are shorter, the overall chrysotile content can reach up to 10%. Areas known as "coarse meshes" contain short and chaotically arranged chrysotile veinlets, separated by sections of hyperbasite. At the periphery of the deposits is the "fine mesh" in fully serpentinized areas of the host rock [48].

The petrographic characteristics of hyperbasites, including their mineralogical composition and texture, play a crucial role in serpentinization processes. These processes, occurring deep within the Earth, lead to the

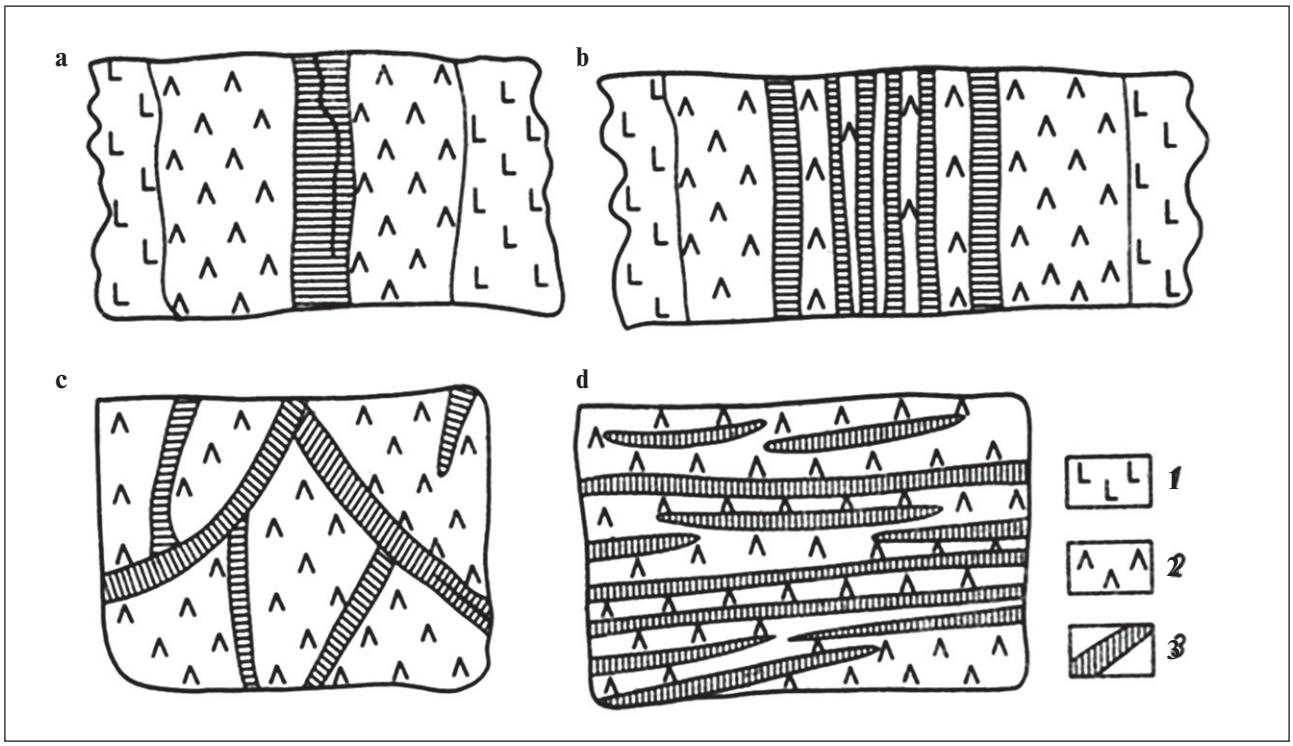

Fig. 2. **Types of chrysotile asbestos veining (textures):** a – simple bordered vein, with a veinlet visible in the center; b – complex bordered vein; c – fine mesh type ore; d – fine vein type ore. 1 – harzburgite, 2 – serpentinite, 3 – chrysotile veins

transformation of primary magmatic minerals into serpentine associations, significantly affecting the asbestos content in these rocks.

Harzburgites, a variety of ultramafic rocks, are often associated with high asbestos content. This is due to their specific mineral composition and formation conditions, which promote the formation of asbestos minerals such as chrysotile. In serpentinized harzburgites, asbestos minerals can form long fibers, making them economically valuable.

The formation of chrysotile asbestos in serpentinized ultramafics is a process that attracts the attention of geologists and environmentalists due to its industrial significance and environmental impact. Chrysotile asbestos, the most common type of asbestos, forms through serpentinization when primary magmatic minerals like olivine and pyroxene transform into serpentine minerals under the influence of water and pressure. These processes not only lead to the formation of chrysotile asbestos but also alter the physical and chemical properties of the original rock, making it less dense and more permeable.

Labinsk deposits form under specific geological conditions characterized by a high degree of serpentinization of ultramafics, resulting in significant reserves of chrysotile asbestos. These deposits have a diverse mineralogical composition, including serpentine minerals, magnesite, talc, and other associated minerals, indicating complex formation processes. Labinsk subtype deposits are distinguished by chrysotile veins with a cross-fiber structure that can extend over long distances [49].

Karachay deposits, like many other types of asbestos deposits, have several unique geological characteristics. One such feature is the presence of longitudinal-fiber veins. The longitudinal-fiber structure of the veins indicates that they formed under conditions where geological forces acted in a specific direction over a significant period. These veins are often rich in asbestos minerals, particularly chrysotile, which is the most common type of asbestos and widely used in industry [50].

Skarn deposits, such as the Aspogash deposit in Russia and their analogs in the USA and China, are contact-metasomatic and associated with serpentinization in dolomitic limestones and dolomites. Asbestos from skarn deposits is characterized by a cross-fiber structure and particularly low iron content, making it especially valuable for the electrical industry due to the high purity and dielectric properties of the material [51].

MATERIALS AND METHODS

Investigating the chemical composition of the constituents of chrysotile cement dust is an important aspect of understanding their environmental and human health impacts. The Quanta 200 3D scanning ion-electron microscope you mentioned is indeed a powerful tool for such studies. It allows not only to visualize micro-objects, but also to analyze their chemical composition with high precision thanks to energy dispersive analysis.

Energy-dispersive analysis (EDA) or X-ray microanalysis (XRMA) utilizes characteristic X-ray emission induced in the sample by an electron beam to determine the elemental composition. This technique enables identification and quantitative assessment of various elements present in the sample.

The focused ion beam system Magnum and the micromanipulator OmniProbe 100.7 enable the extraction and preparation of thin foils from specific regions of the sample, which is necessary for transmission electron microscopy. This facilitates obtaining more detailed information about the structure and composition of the material.

The localized tungsten deposition system "W deposition" and the integrated Pegasus 2000 system for microanalysis with the Sapphire X-ray detector enhance the capabilities of the microscope, enabling more complex studies, including the determination of grain misorientation using backscattered electron diffraction.

Two varieties of spectrometers are used to investigate spectral features within RSMa: one without the use of a crystal and one with a crystal analyzer. These devices provide high accuracy in determining the composition of elements in the samples, which is critical for studying the characteristics of chrysotile cement dust and assessing its effects.

The chrysotile-cement dust used in the study was obtained from the production line of the first slate plant of the "BelACI" company. Dust collection took place during the sawing process of chrysotile-cement products, after which it was dispersed using a centrifugal separator. The sample was stored in polyethylene containers with a self-sealing lid.

In the experiment to analyze the effect of acidity on the structure of initial commercial fibers of chrysotile cement dust, solutions with different pH levels: 3, 4, and 6 were used. The procedure included placing 1 gram of dust in a test tube followed by the addition of 20 ml of HCl solution. The solutions were prepared by diluting 60 ml of distilled water with 10 ml of 0.1M HCl to achieve pH 3, 5 ml for pH 4, and 2.5 ml for pH 6. The samples were kept in these environments for 2 hours, 24 hours, three days, and a week at 30°C. Afterwards, the samples were washed with water and analyzed using the scanning ion-electron microscope at magnifications of 200×, 500×, 5000×, and 10000× to study their chemical composition.

RESULTS

Based on the obtained images taken with the electron microscope, a visual analysis was performed to determine the number of individual fibers and their clusters. The data are presented in Table 1.

Table 1
Quantitative composition of initial commercial fibers and their aggregates in chrysotile cement dusts

No. of p.p.	Number of fibrous particles in asbestos–cement dust at visual counting in electron microscope, pcs.								
	Fiber aggregates					Fibers			
	Aging time in acidic medium	augmentation				augmentation			
		200x	500x	5000x	10000x	200x	500x	5000x	10000x
Initial chrysotile cement dust (dispersed powder)									
1	–	5	5	4	5	11	7	6	7
	Initial chrysotile cement dust in acidic medium (PH = 3)								
1	2 hours	2	2	2	7	8	7	5	5
2	1 day	–	–	1	3	5	8	8	8
3	3 days	–	2	1	–	9	13	60	80
4	1 week	–	1	–	2	5	15	90	100
Initial chrysotile cement dust in acidic medium (PH = 4)									
1	2 hours	1	2	2	1	6	19	40	180
2	1 day	–	1	1	–	4	16	80	150
3	3 days	–	1	2	–	15	15	50	100
4	1 week	–	1	1	–	8	10	90	100
Initial chrysotile cement dust in acidic medium (PH = 6)									
1	2 hours	–	1	1	–	7	9	30	150
2	1 day	2	1	1	1	15	13	50	60
3	3 days	1	–	–	–	12	16	50	70
4	1 week	–	–	–	1	9	20	150	100

* – The fiber count was performed using 10 photographs for each sample

Table 2
Chemical composition of chrysotile cement dust and after its exposure in acidic medium

№	Medium acidity	Exposure time	Oxide content,wt.%						
			MgO	SiO_2	SO_3	K_2O	CaO	Fe_2O_3	NiO
1	Initial asbestos-cement dust (powder)		22.71	33.3	2.34	0.59	38.1	2.96	–
2	PH = 3	2 hours	19.85	33.88	1.57	0.57	41.47	2.66	–
3		1 day							–
4		3 days	13.79	29.77	2.12	0.55	49.65	4.12	–
5		1 week	21.30	35.00	1.93	0.63	38.11	3.03	–
6	PH = 4	2 hours	22.66	34.28	1.98	0.54	38.08	2.46	–
7		1 day	23.27	34.75	2.24	0.53	36.12	3.1	–
8		3 days	19.71	35.33	2.3	0.44	39.52	2.71	–
9		1 week	14.57	29.6	2.47	0.51	49.19	3.65	–
10	PH = 6	2 hours	20.30	31.07	2.80	0.64	41.83	3.36	–
11		1 day	8.96	25.35	2.54	–	55.45	7.03	0.66
12		3 days	26.47	36.05	1.5	–	33.81	2.17	–
13		1 week	11.12	30.16	2.75	–	51.99	3.99	–

The study of the data presented in Table 1 showed that after exposure to an acidic environment, the number of fiber aggregates in the chrysotile-cement dust decreased by 20–40 units, while the number of individual thin fibers increased by 10–900 units. This change in the quantity of fibers and aggregates is due to the breakdown of the cement matrix surrounding the chrysotile fibers, leading to the disintegration of parallel-fiber aggregates of chrysotile in an acidic environment.

The chemical composition of the fibers, including both the original chrysotile-cement dust and the samples exposed to acid for 2 hours, 1 day, 3 days, and 1 week at pH levels 3, 4, and 6 and a temperature of 30°C, is detailed in Table 2.

DISCUSSION

The study of the chemical composition of chrysotile cement dust exposed to acid allows us to conclude that there is an increase in the level of calcium oxide (CaO) on the surface of microfibers. This phenomenon is due to the adsorption of CaO from the solution, which is leached out from the hydration products of Portland cement during the leaching process.

Electron microscope images and microdiffraction patterns of the fibrous component of the cement dust at different pH levels are shown in Figures 3–6, respectively.

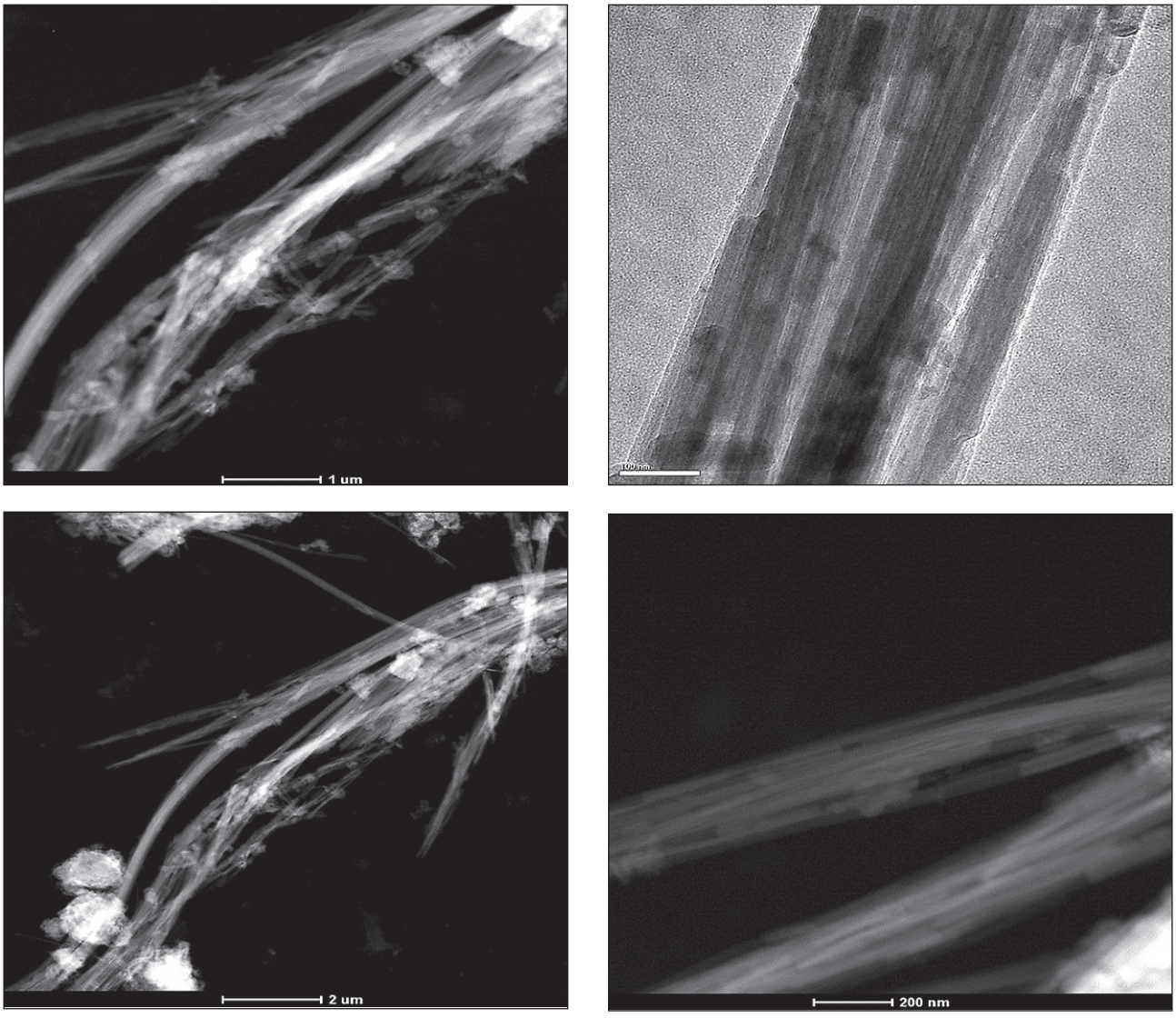

Fig. 3. **Chrysotile micro- and nanofibers in samples of chrysotile cement dust after its soaking in acidic medium at PH = 4 for 2 hours**

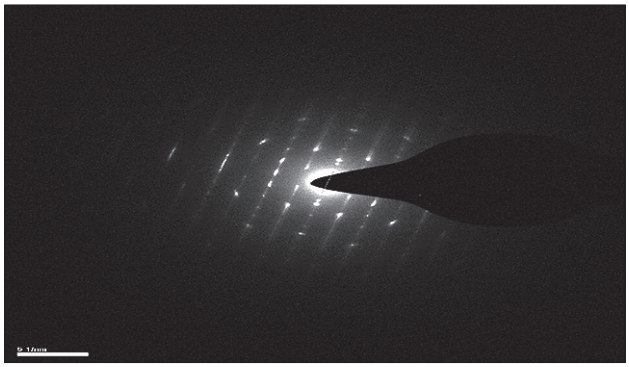

Fig. 4. **Microdiffraction pattern of chrysotile cement dust nanofibers aged in acidic medium at PH = 4 for 2 hours**

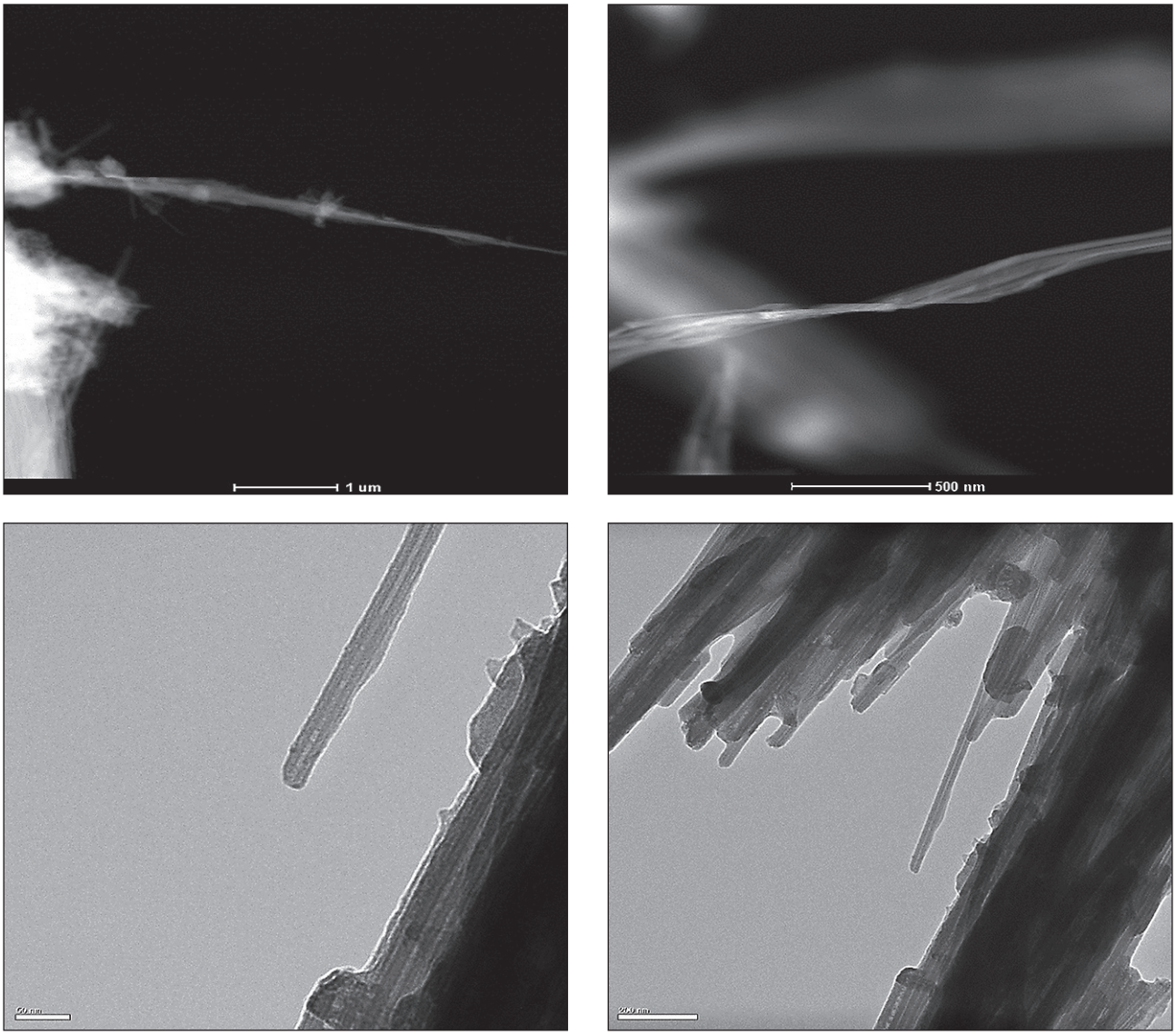

Fig. 5. **Chrysotile micro- and nanofibers in samples of chrysotile cement dust after its soaking in acidic medium at PH = 4 for 1 week**

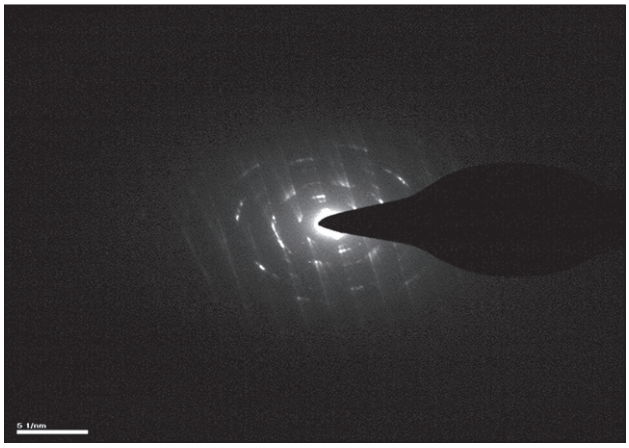

Fig. 6. **Microdiffraction pattern of chrysotile cement dust nanofibers aged in acidic medium at PH = 4 for 1 week**

Table 3

Chemical composition of chrysotile-cement dust after exposure to an acidic environment based on energy-dispersive microanalysis data

№	Acidity medium	Exposure time	Oxide content,wt.%			
			MgO	SiO_2	CaO	Fe_2O_3
1	PH = 4	2 hours	19.82	33.75	3.18	
2		1 week	5.67	46.06	4.79	0.39

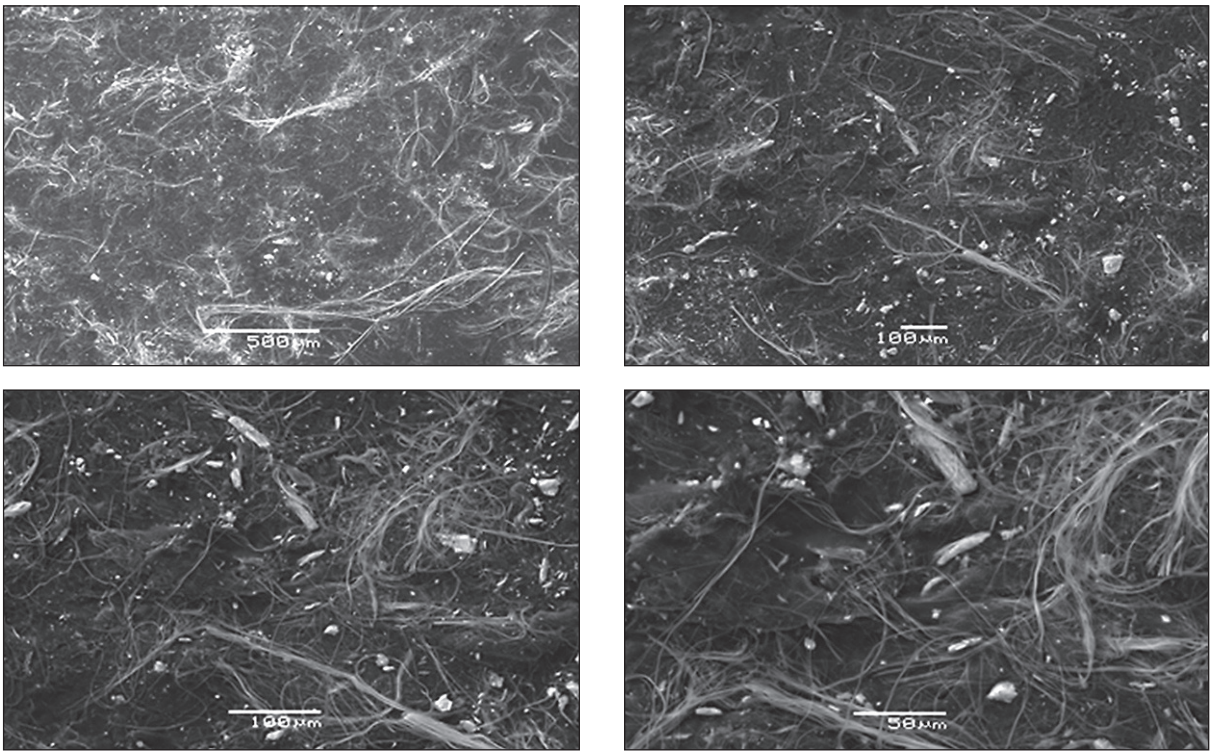

Fig. 7. **Microfibers and fiber bundles of commercial chrysotile in chrysotile cement dusts**

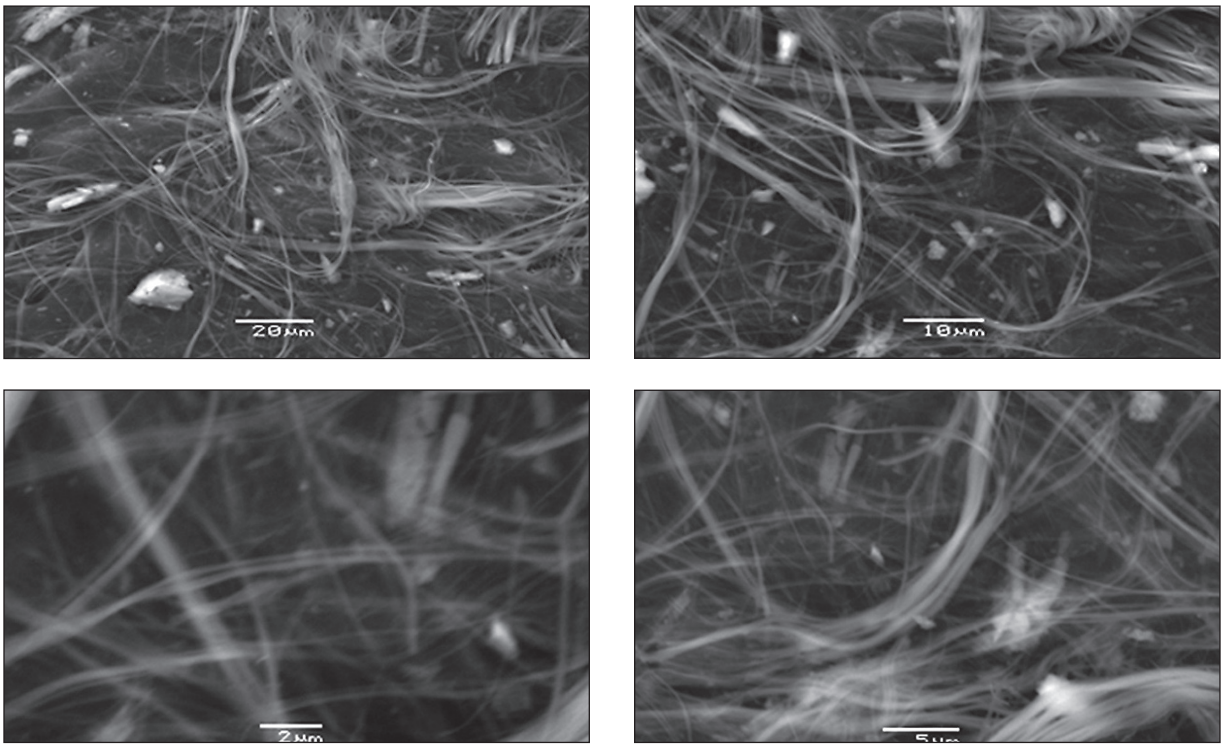

Fig. 7. **The End**

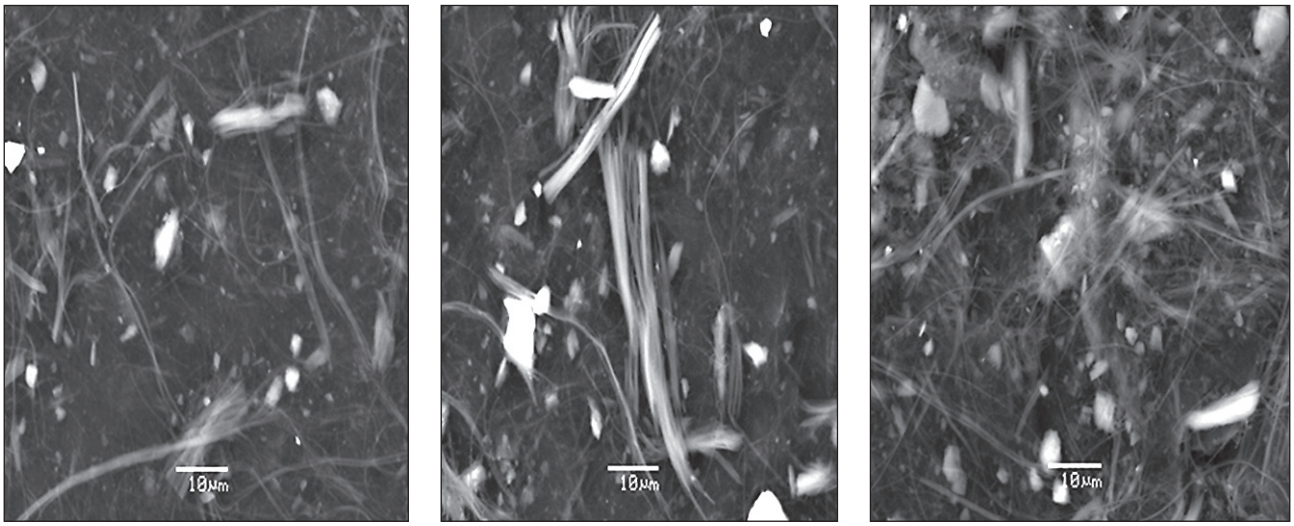

Fig. 8. **Microfibers and fiber bundles of chrysotile cement dust**

Table 4
The number of different particles in samples from chrysotile-cement dust and commercial chrysotile based on images of specimens from aqueous suspensions

No. of p.p.	Type and number of particles									
	Total	Fibrous							Granular	
		Together fibers and bundles		Separate fibers		Separate bundles				
	pcs.	pcs.	% absolute	pcs.	% relative to the sum of all particles	pcs.	% отн, от суммы		pcs.	% absolute
							all particles	fibers		
A/c										
1	799	332	45,6	327	41,0	37	4,6	10,2	435	54,4
A product										
2	867	482	55,6	424	48,9	58	6,7	12,0	385	44,4

Table 5
Distribution of length sizes of chrysotile fibers longer than 150 μm

Units of measurement	Number of fibers of different lengths					
Mkm	up to150	150–200	200–250	250–300	300–350	350–400
A/c						
%,absolute	95.7	0.9	2.5	0.6	0.9	–
%,total	95.7	96.6	99.1	99.7	100.0	–
A product						
%,absolute	95.4	1.2	1.7	0.6	0.3	0.2
%,total	95. 4	96.6	98.3	98.9	99.8	100.0

Table 6
Quantity and sizes of granular particles

Units of measurement	Number of particles of different sizes			
micrometer	from 1×1 to 2×2	from 3×3 to 6×10	from 10×18 to 15×15	from 20×30 to 100×120
A/c				
%,absolute	81	13	–	6
%,total	81	94	–	100
A product				
%,absolute	84	15	1	–
%,total	84	99	100	–

Table 7
Chemical composition of initial chrysotile and chrysotile exposed to hardened Portland cement

No. of p.p.	Chrysotile asbestos oxide content, absolute %						
	MgO	Al_2O_3	SiO_2	Fe_2O_3	CaO	CuO	SO_3
A/c							
1	39.54	0.43	43.04	1.41	15.01	–	0.57
A product							
2	45.25	0.73	48.58	3.85	0.89	0.1	–

Microfibers of commercial chrysotile and their bundles in chrysotile cement dust are presented in Fig. 7 and 8.

CONCLUSIONS

The study of the chemical composition of nanofibers and fiber bundles of chrysotile-cement dust in an acidic environment represents a significant contribution to understanding the effects of acidity on chrysotile-cement materials. The use of the Quanta 200 3D scanning ion-electron microscope and energy-dispersive analysis allowed for precise determination of changes in the quantitative and chemical composition of nanofibers and their bundles after exposure to an acidic environment and the hydration products of Portland cement.

The results show that exposure to an acidic environment leads to a decrease in the number of fiber aggregates and an increase in the number of nanofibers. This change may be due to the destruction of the cement matrix covering the chrysotile fibers, leading to the dispersion of parallel-fiber aggregates of chrysotile. Chemical analysis revealed an increase in the calcium oxide content on the surface of nanofibers and their bundles, which may result from its sorption from the solution during leaching from the hydration products of Portland cement.

Thus:

– it is shown, how fibers of initial commercial chrysotile extracted from dunite-harzburgite rocks of Bazhenov deposit and used at manufacture of chrysotile cement products behave.
– electron microscopic estimation of quality of initial commercial chrysotile fibers and their bundles in cement component and after their processing in medium with different acidity was carried out.

The received results will allow to use natural and technogenic raw materials in manufacture of filled composite materials.

REFERENCES

1. Zayed A.M., El-Khayatt A.M., Petrounias P., Shahien M.G., Mahmoud K.A., Rashad A.M., et al. From discarded waste to valuable products: Barite combination with chrysotile mine waste to produce radiation-shielding concrete. Constr Build Mater 2024;417:135334. https://doi.org/10.1016/j.conbuildmat.2024.135334

2. Shkarednaya S.A., Kaskevich T.M. Asbestos-containing products and building materials. 2005; 2:37 – 39.

3. Akylbekov Y., Shevko V., Karatayeva G. Thermodynamic prediction of the possibility of comprehensive processing chrysotile-asbestos waste. Case Stud Chem Environ Eng 2023;8:100488. https://doi.org/10.1016/j.cscee.2023.100488

4. Cai N., Wang K., Li N., Huang S., Xiao Q. Novel sandwich structured chrysotile fiber separator for advanced lithium-ion batteries. Appl Clay Sci 2019;183:105327. https://doi.org/10.1016/j.clay.2019.105327

5. Radvanec M., Tuček Ľ., Derco J., Čechovská K., Németh Z. Change of carcinogenic chrysotile fibers in the asbestos cement (eternit) to harmless waste by artificial carbonatization: Petrological and technological results. J Hazard Mater 2013;252–253:390–400. https://doi.org/10.1016/j.jhazmat.2013.02.036

6. Gualtieri A.F., Bursi Gandolfi N., Pollastri S., Burghammer M., Tibaldi E., Belpoggi F., et al. New insights into the toxicity of mineral fibres: A combined in situ synchrotron μ-XRD and HR-TEM study of chrysotile, crocidolite, and erionite fibres found in the tissues of Sprague-Dawley rats. Toxicol Lett 2017;274:20–30. https://doi.org/10.1016/j.toxlet.2017.04.004

7. Wronkiewicz S.K., Roggli V.L., Hinrichs B.H., Kendler A., Butler R.A., Christensen B.C., et al. Chrysotile fibers in tissue adjacent to laryngeal squamous cell carcinoma in cases with a history of occupational asbestos exposure. Mod Pathol 2020;33:228–34. https://doi.org/10.1038/s41379-019-0332-7

8. Lemen R.A., Wagner G.R. Asbestos. Ref. Modul. Biomed. Sci., Elsevier; 2024. https://doi.org/10.1016/B978-0-323-99967-0.00192-7

9. Kuhta T.N. Enhancing the durability of polymer coatings on asbestos-cement sheets using a water repellent. Construction Materials. 2010; 1: 58 – 60

10. Tan Y., Zou Z., Qu J., Ren J., Wu C., Xu Z. Mechanochemical conversion of chrysotile asbestos tailing into struvite for full elements utilization as citric-acid soluble fertilizer. J Clean Prod 2021;283:124637. https://doi.org/10.1016/j.jclepro.2020.124637

11. Fedyuk R.S., Lesovik V.S., Liseitsev Yu.L., Timokhin R.A., Bituev A.V., Zayakhanov M.I., et al. Composite binders for concrete with increased impact resistance. Engineering and Construction Journal, 2019. 85. 28-38. https://doi.org/10.18720/MCE.85.3

12. Valouma A., Verganelaki A., Maravelaki-Kalaitzaki P., Gidarakos E. Chrysotile asbestos detoxification with a combined treatment of oxalic acid and silicates producing amorphous silica and biomaterial. J Hazard Mater 2016;305:164–70. https://doi.org/10.1016/j.jhazmat.2015.11.036.

13. Klyuyev S.V., Klyuyev A.V., Sopin D.M., Netrebenko A.V., Kazlitin S.A. Heavy loaded floors based on fine-grained fiber concrete. Magazine of Civil Engineering. 2013;38(3):7–14.

14. Sambueva S.R., Batomunkueva Ts.D.D. Structural parameters of YBa2Cu3-xO6+y. Chemical Bulletin. 2024; 7 (1): 41 – 48. https://doi.org/10.58224/2619-0575-2024-7-1-41-48

15. Nel A. Carbon nanotube pathogenicity conforms to a unified theory for mesothelioma causation by elongate materials and fibers. Environ Res 2023;230:114580. https://doi.org/10.1016/j.envres.2022.114580

16. Gualtieri A.F., Malferrari D., Di Giuseppe D., Scognamiglio V., Sala O., Gualtieri M.L., et al. There is plenty of asbestos at the bottom. The case of magnesite raw material contaminated with asbestos fibres. Sci Total Environ 2023;898:166275. https://doi.org/10.1016/j.scitotenv.2023.166275

17. Peng Q., Dai Y., Liu K., Tang X., Zhou M., Zhang Y., et al. Outstanding catalytic performance of metal-free peroxymonosulfate activator: Important role of chrysotile. Sep Purif Technol 2022;287:120526. https://doi.org/10.1016/j.seppur.2022.120526

18. Xing J., Peng Q., Zhong W., Zhang Y., Wang X., Liu K. Highly efficient activation of peroxymonosulfate by novel CuO-Chrysotile catalytic membrane for degradation of p-nitrophenol. J Water Process Eng 2023;51:103403. https://doi.org/10.1016/j.jwpe.2022.103403

19. Lyakishev V.K., Perfilyev M.S. Quantum model of anharmonic vibrations of a diatomic molecule with a variable force constant and a small value of the anharmonicity coefficient. Chemical Bulletin. 2024. 7 (1). P. 22 – 31. https://doi.org/10.58224/2619-0575-2024-7-1-22-31

20. Fantone S., Tossetta G., Cianfruglia L., Frontini A., Armeni T., Procopio A.D., et al. Mechanisms of action of mineral fibres in a placental syncytiotrophoblast model: An in vitro toxicology study. Chem Biol Interact 2024;390:110895. https://doi.org/10.1016/j.cbi.2024.110895

21. Fediuk R., Smoliakov A., Stoyushko N. Increase in composite binder activity. IOP Conf. Ser. Mater. Sci. Eng., vol. 156, 2016. https://doi.org/10.1088/1757-899X/156/1/012042

22. Yoshida N., Saeki Y. Chrysotile fibers penetrate Escherichia coli cell membrane and cause cell bursting by sliding friction force on agar plates. J Biosci Bioeng 2004;97:162–8. https://doi.org/10.1016/S1389-1723(04)70186-3

23. Masoud M.A., El-Khayatt A.M., Mahmoud K.A., Rashad A.M., Shahien M.G., Bakhit B.R., et al. Valorization of hazardous chrysotile by H3BO3 incorporation to produce an innovative eco-friendly radiation shielding concrete: Implications on physico-mechanical, hydration, microstructural, and shielding properties. Cem Concr Compos 2023;141:105120. https://doi.org/10.1016/j.cemconcomp.2023.105120

24. Bernstein D.M., Toth B., Rogers R.A., Kunzendorf P., Phillips J.I., Schaudien D. Final results from a 90-day quantitative inhalation toxicology study evaluating the dose-response and fate in the lung and pleura of chrysotile-containing brake dust compared to TiO2, chrysotile, crocidolite or amosite asbestos: Histopathological examinat. Toxicol Appl Pharmacol 2021;424:115598. https://doi.org/10.1016/j.taap.2021.115598

25. Chagarova O.V., Milinsky A.Yu., Kositsyna O.A. Application of thermal methods for the analysis of organic matter content in urbanozems. Chemical Bulletin. 2024. 7 (1). P. 32 – 40. https://doi.org/10.58224/2619-0575-2024-7-1-32-40

26. Abbasi M., Hosseiny B., Stewart R.A., Kalantari M., Patorniti N., Mostafa S., et al. Multi-temporal change detection of asbestos roofing: A hybrid object-based deep learning framework with post-classification structure. Remote Sens Appl Soc Environ 2024;34:101167. https://doi.org/10.1016/j.rsase.2024.101167

27. Bernasconi A., Pellegrino L., Vergani F., Campanale F., Marian N.M., Galimberti L., et al. Recycling detoxified cement asbestos slates in the production of ceramic sanitary wares. Ceram Int 2023;49:1836–45. https://doi.org/10.1016/j.ceramint.2022.09.147

28. Saba M., Torres Gil L.K., Chanchí Golondrino G.E. Physicochemical analysis of primers and liquid membranes as asbestos' encapsulant. Constr Build Mater 2023;409:133972. https://doi.org/10.1016/j.conbuildmat.2023.133972

29. Ranaivomanana H., Leklou N. Investigation of microstructural and mechanical properties of partially hydrated Asbestos-Free fiber cement waste (AFFC) based concretes: Experimental study and predictive modeling. Constr Build Mater 2021;277:121943. https://doi.org/10.1016/j.conbuildmat.2020.121943

30. Punenkov S.E. Composites materials based on natural chrysotile fibers. Chemical Bulletin. 2024. 7 (1). P. 4 – 21. https://doi.org/10.58224/2619-0575-2024-7-1-4-21

31. Klyuyev S.V., Kashapov N.F., Radaykin O.V., Sabitov L.S., Klyuyev A.V., Shchekina N.A. Reliability coefficient for fibreconcrete material. Construction Materials and Products 2022;5:51–58. https://doi.org/10.34031/2618-7183-2022-5-2-51-58

32. Boffetta P., Righi L., Ciocan C., Pelucchi C., La Vecchia C., Romano C., et al. Validation of the diagnosis of mesothelioma and BAP1 protein expression in a cohort of asbestos textile workers from Northern Italy. Ann Oncol 2018;29:484–9. https://doi.org/10.1093/annonc/mdx762

33. Sabat M., Fares N., Mitri G., Kfoury A. Determination of asbestos cement rooftop surface composition using regression analysis and hyper-spectral reflectance data in the visible and near-infrared ranges. J Hazard Mater 2024;469:134006. https://doi.org/10.1016/j.jhazmat.2024.134006

34. Klyuyev S.V., Guryanov Yu.V. External reinforcing of fiber concrete constructions by carbon fiber tapes. Magazine of Civil Engineering. 2013; 36(1):21–26.

35. Feletto E., Schonfeld S.J., Kovalevskiy E .V., Bukhtiyarov I.V., Kashanskiy S.V., Moissonnier M., et al. A comparison of parallel dust and fibre measurements of airborne chrysotile asbestos in a large mine and processing factories in the Russian Federation. Int J Hyg Environ Health 2017;220:857–68. https://doi.org/10.1016/j.ijheh.2017.04.001

36. Bridle J., Hoskins J. Canadian hypocrisy regarding chrysotile. Lancet 2011;377:720. https://doi.org/10.1016/S0140-6736(11)60271-7

37. Punenkov S.E., Kozlov Yu.S. Chrysotile asbestos and resource conservation in the chrysotile asbestos industry. Mining Journal of Kazakhstan. 2022; 1: 5 – 10.

38. Chaumba J.B., Mamuse A. Petrographic and mineral chemistry investigation of the high-grade chrysotile asbestos-bearing Zvishavane Ultramafic Complex, south central Zimbabwe. Geochemistry 2023;83:125950. https://doi.org/10.1016/j.chemer.2023.125950

39. Biondi J.C. Neoproterozoic Cana Brava chrysotile deposit (Goiás, Brazil): Geology and geochemistry of chrysotile vein formation. Lithos 2014;184–187:132–54. https://doi.org/10.1016/j.lithos.2013.10.017

40. Kuznetsov D.V., Klyuev S.V., Ryazanov A.N., Sinitsin D.A., Pudovkin A.N., Kobeleva E.V., Nedoseko I.V. Dry mixes on gypsum and mixed bases in the construction of low-rise residential buildings using 3D printing technology. Construction Materials and Products. 2023. 6 (6). 5. https://doi.org/10.58224/2618-7183-2023-6-6-5

41. Klyuev A.V., Kashapov N.F., Klyuev S.V., Lesovik R.V., Ageeva M.S., Fomina E.V. Development of alkali-activated binders based on technogenic fibrous materials. Construction Materials and Products. 2023; 6 (1): 60–73. https://doi.org/10.58224/2618-7183-2023-6-1-60-73

42. Klyuev A.V., Kashapov N.F., Klyuev S.V., Zolotareva S.V., Shchekina N.A., Shorstova E.S., Lesovik R.V., Ayubov N.A. Experimental studies of the processes of structure formation of composite mixtures with technogenic mechanoactivated silica component. Construction Materials and Products. 2023; 6 (2):5 – 18. https://doi.org/10.58224/2618-7183-2023-6-2-5-18

43. Hodel F., Macouin M., Triantafyllou A., Carlut J., Berger J., Rousse S., et al. Unusual massive magnetite veins and highly altered Cr-spinels as relics of a Cl-rich acidic hydrothermal event in Neoproterozoic serpentinites (Bou Azzer ophiolite, Anti-Atlas, Morocco). Precambrian Res 2017;300:151–67. https://doi.org/10.1016/j.precamres.2017.08.005

44. Naumova L.N. Influence of acidic environment on the properties of chrysotile-cement dust. Bulletin of BSTU named after V.G. Shukhov 2011 ; 2 : 24-27.

45. Portella Y de M., Conceição R.V., Siqueira T.A., Gomes L.B., Iglesias R.S. Experimental evidence of pressure effects on spinel dissolution and peridotite serpentinization kinetics under shallow hydrothermal conditions. Geosci Front 2024;15:101763. https://doi.org/10.1016/j.gsf.2023.101763

46. Wang L., Xiong Q., Zheng J-P., Dai H-K., Tian L-R., Zhou X. Multistage and diverse melt-mantle interaction in dunite-harzburgite channel systems beneath oceanic slow-ultraslow spreading centers: Evidence from the Xigaze ophiolite (Tibet). Lithos 2024;468–469:107501. https://doi.org/10.1016/j.lithos.2024.107501

47. Capitani G., Dalpiaz M., Vergani F., Campanale F., Conconi R., Odorizzi S. Recycling thermally deactivated asbestos cement in mortar: A possible route towards a rapid conclusion of the "asbestos problem." J Environ Manage 2024;355:120507. https://doi.org/10.1016/j.jenvman.2024.120507

48. Fitzgerald S.M. Resolving asbestos and ultrafine particulate definitions with carcinogenicity. Lung Cancer 2024:107478. https://doi.org/10.1016/j.lungcan.2024.107478

49. Jefferson I.F., Evstatiev D., Karastanev D., Mavlyanova N.G., Smalley I.J. Engineering geology of loess and loess-like deposits: a commentary on the Russian literature. Eng Geol 2003;68:333–51. https://doi.org/10.1016/S0013-7952(02)00236-3

50. Okrostsvaridze A., Chung S-L., Lin Y-C., Skhirtladze I. Geology and zircon U-Pb geochronology of the Mtkvari pyroclastic flow and evaluation of destructive processes affecting Vardzia rock-cut city, Georgia. Quat Int 2020;540:137–45. https://doi.org/10.1016/j.quaint.2019.03.026

51. Liu W., Wan B. Carbon flux from hydrothermal skarn ore deposits and its potential impact to the environment. Gondwana Res 2024;126:343–54. https://doi.org/10.1016/j.gr.2023.09.017

INFORMATION ABOUT THE AUTHORS

Sergey V. Klyuyev – Dr. Sci. (Eng.), Professor, Patrice Lumumba Peoples' Friendship University of Russia, Belgorod State Technological University named after V.G. Shukhov, Belgorod, Russia, klyuyev@yandex.ru, https://orcid.org/0000-0002-1995-6139

Lyudmila N. Naumova – Cand. Sci. (Eng.), Associate Professor, Belgorod State Technological University named after V.G. Shukhov, Belgorod, Russia, naymova_ln@mail.ru, https://orcid.org/0000-0003-4822-3767

Igor V. Nedoseko – Dr. Sci. (Eng.), Professor, Ufa State Petroleum Technological University, Ufa, Russia, nedoseko1964@mail.ru, https://orcid.org/0000-0001-6360-6112

Alexander V. Klyuyev – Cand. Sci. (Eng.), Associate Professor of the Department of "Theoretical Mechanics and Strength of Materials", Belgorod State Technological University named after V.G. Shukhov, Belgorod, Russia, megastaryj@yandex.ru, https://orcid.org/0000-0003-0845-8414

Elena S. Shorstova – Cand. Sci. (Eng.), Associate Professor of the Department of "Theoretical Mechanics and Strength of Materials", Belgorod State Technological University named after V.G. Shukhov, Belgorod, Russia, kuzik_alena@mail.ru, https://orcid.org/0000-0003-4031-0989

CONTRIBUTION OF THE AUTHORS

The authors contributed equally to this article.

The authors declare no conflicts of interests.

The article was submitted 08.07.2024; approved after reviewing 07.08.2024; accepted for publication 14.08.2024.